Chapter 1

Fundamentals of Grain Boundaries and Triple Lines

1.1 Introdution

Real metals and alloys are never free of defects. This is a common agreement in the field of material science and engineering. Since materials are basically in the form of polycrystals in practice, classical defects such as vacancies, dislocations, planar boundaries, and the new ones, facets and ridges on the boundaries are actually the structural elements of a polycrystal.

Grain boundaries, which separate two regions of the same crystallographic structure but of different orientations, are one of the most important microstructural elements [Gottstein 2010a]. The thermodynamics and kinetics of grain boundaries have been addressed frequently in the past, as they play a significant role in most thermo-mechanical processes and impact the material properties, such as strength, corrosion resistance and so on. However grain boundary triple junctions, i.e. the intersection of grain boundaries to form a contiguous arrangement of grains in a polycrystal, are often overlooked as being part of the connecting grain boundaries. Grain boundary triple junctions are 1-dimensional microstructural elements on their own with specific thermodynamic and kinetic properties, which require an understanding of the attached grain boundaries as well as advanced physical and mathematical description tools for their investigation and characterization.

1.2 Grain boundaries

1.2.1 Grain boundary structure

In real systems (a three-dimensional case), it needs eight parameters to unambiguously describe a grain boundary. Three terms are for the specific orientation difference between the two adjacent grains, which can be presented by the Euler angles (φ_1, Φ, φ_2), by Miller indices or by an angle-axis pair in the Rodrigues-Frank space [Rodrigues 1840; Frank 1988]. Two parameters are for the spatial orientation of the grain boundary by means of the normal to the grain boundary plane, i.e. the inclination plane, given by the normal unit vector $\mathbf{n} = (n_1, n_2, n_3)$ with regard to one of the adjacent grains. In addition to the five macroscopic parameters referred, three microscopic parameters are required to describe the displacement of one crystal with respect to the other, given by the translational vector $\mathbf{t} = (t_1, t_2, t_3)$. The intrinsic properties of a grain boundary, in particular the grain boundary mobility and energy, are principally a function of the eight parameters.

The orientation relationship between two crystal lattices, i.e. misorientation, is actually a transformation, which is applied to one crystal to make both crystal lattices coincide. If a common origin for both crystal lattices is assumed, this transformation is a pure rotation of one crystal coordinate system with regard to the other. Hence, the easiest way to discriminate different kinds of grain boundaries is to present the rotation in terms of a crystallographic axis <*hkl*> or a vector [*uvw*] and a rotation angle φ. For example, if the grain boundary plane is perpendicular to the rotation axis, the grain boundary is referred to as a pure twist grain boundary (Fig. 1.1a). In such a case the grain boundary plane is clearly defined, no matter what the rotation angle is. In contrast, it is called a pure tilt grain boundary when its rotation axis is within the grain boundary plane. In the case of tilt grain boundaries, there is an infinite number of possible grain boundary planes for a give rotation angle. If the two adjacent grains have a mirror symmetry, it is the simplest type of grain boundary, referred to as a symmetric tilt grain boundary (Fig. 1.1b). All other tilt grain boundaries are identified as asymmetrical tilt grain boundaries (Fig. 1.1c).

Apart from the above classification of the grain boundaries, it is also possible to distinguish two different kinds of grain boundaries: low angle grain boundaries (LAGB) and high angle grain boundaries (HAGB), depending on the magnitude of the rotation angle φ between adjacent grains.

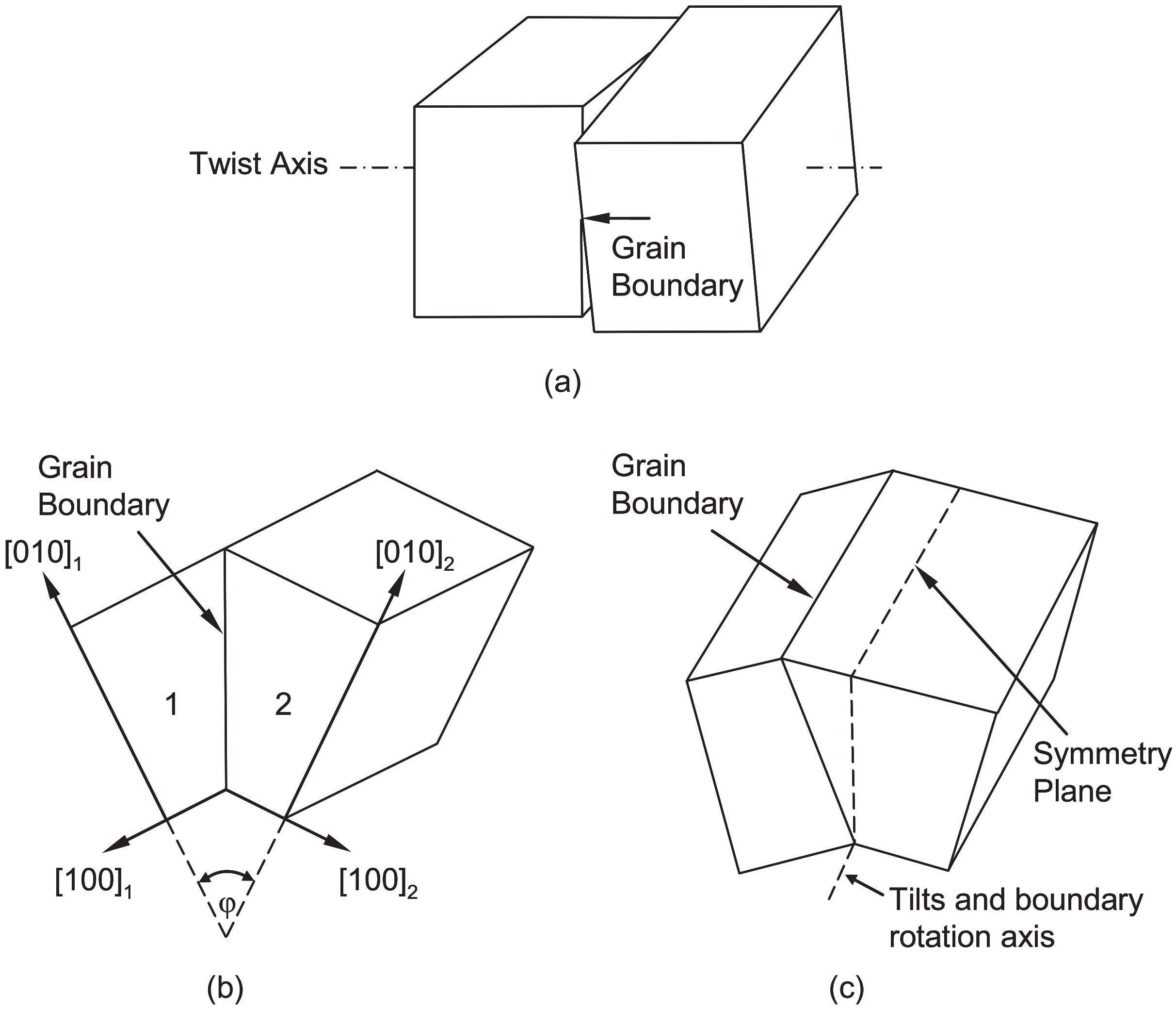

Fig. 1.1: Relative orientation of grain boundaries and rotation axes for different types of grain boundaries: (a) Twist grain boundary; (b) symmetrical tilt grain boundary; (c) asymmetrical tilt grain boundary [Gottstein 2010a].

Low Angle Grain boundaries

If the rotation angle φ does not exceed 15°, it is normally assumed that the grain boundary is completely comprised of a periodic crystal dislocation arrangement. In Fig. 1.2, it is shown the configuration of a symmetric <100> low angle tilt grain boundary, consisting of a single set of edge dislocations with the same Burgers vector b. The dislocation spacing d is directly connected with the rotation angle φ (Fig. 1.2a),

$$\frac{b}{d} = 2\sin\frac{\varphi}{2} \approx \varphi \tag{1.1}$$

The dislocation spacing d increases with decreasing rotation angle φ (Fig. 1.2b).

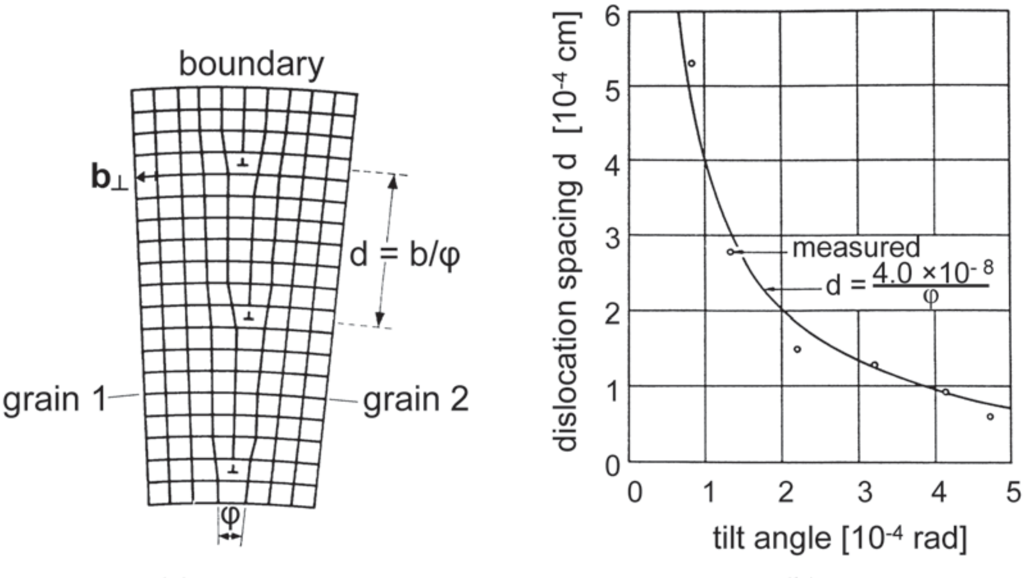

(a) (b)

Fig. 1.2: (a) Dislocation configuration of a symmetrical <100> low angle grain boundary with tilt angle *φ* in a simple cubic crystal; (b) Measured and calculated dislocation spacing in a symmetrical low angle tilt boundary in germanium [Gottstein 2010a].

In the general case, an asymmetrical tilt grain boundary can be assumed as a deviation from a symmetrical tilt grain boundary, which needs a new set of dislocations to compensate the deviation (inclination) Φ (Fig. 1.3). Hence, an asymmetrical tilt grain boundary configuration requires at least two sets of edge dislocations, the Burgers vectors of which are perpendicular to each other. The number of the new set of dislocations increases with increasing deviation. The dislocation spacing d_1 and d_2 of the first set with Burgers vectors b_1 and the second set b_2 are given by

$$\frac{1}{d_1} = \frac{b_1}{\varphi \cos \Phi} \tag{1.2}$$

$$\frac{1}{d_2} = \frac{b_2}{\varphi \sin \Phi} \tag{1.3}$$

By contrast, low angle twist grain boundaries require at least two sets of screw dislocations and mixed low angle grain boundaries are comprised by dislocation networks of three Burgers vector [Read 1950]. The dislocation model by Read and Shockley predicts exactly the energy increase with rising angle of rotation *φ* for low angle grain boundary, and is supported by experimental measurements of grain boundary energy [Smith 1976].

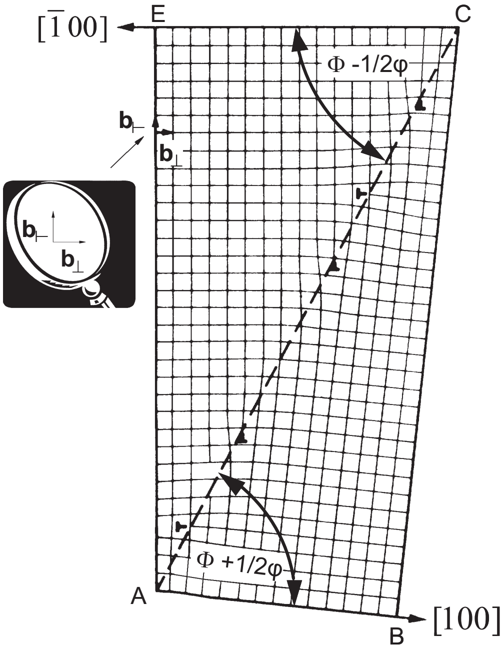

Fig. 1.3: Dislocation configuration of an asymmetrical low angle tilt grain boundary with tilt angle φ and inclination Φ [Gottstein 2010a].

High Angle Grain boundaries

The dislocation model succeeds due to the assumption that the dislocation spacing d is so large that the interaction between the dislocation cores is negligible. However, the dislocation spacing d decreases with increasing rotation angle φ according to Eq. (1.1). For the rotation angle φ >15°, the dislocation cores begin to overlap each other, and lose their identity as individual lattice defects. Therefore, grain boundaries of misorientation angle in excess of 15° are termed high angle grain boundaries, the structures of which are distinguished from low angle grain boundaries.

A common method of the structure description of high angle grain boundaries is still based on the dislocation model of low angle grain boundaries. The atomic positions in a perfect crystal are determined by the minimum of the free energy. Any deviation from the defined positions will inescapably introduce a free energy increase. Consequently, it can be assumed that the atoms in the grain boundary will tend to stay in the ideal positions (low energetic positions). At special misorientations, there are crystallographic planes, which continue through the grain boundary from one crystal to the other, i.e. certain atomic positions in the grain boundary coincide with ideal positions of both adjacent crystal lattices. Such lattice points are termed coincidence sites. Since the orientation relationship between the adjacent grains can be described by a rotation, it can be analyzed under what conditions such coincidence sites will occur. A typical example is the rotation of 36.87° about a <100> axis in a cubic lattice (Fig. 1.4a). Due to the periodicity of the crystal lattices of both grains, the coincidence sites are also periodic. The lattice built by the coincidence sites is termed the Coincidence Site Lattice (CSL).

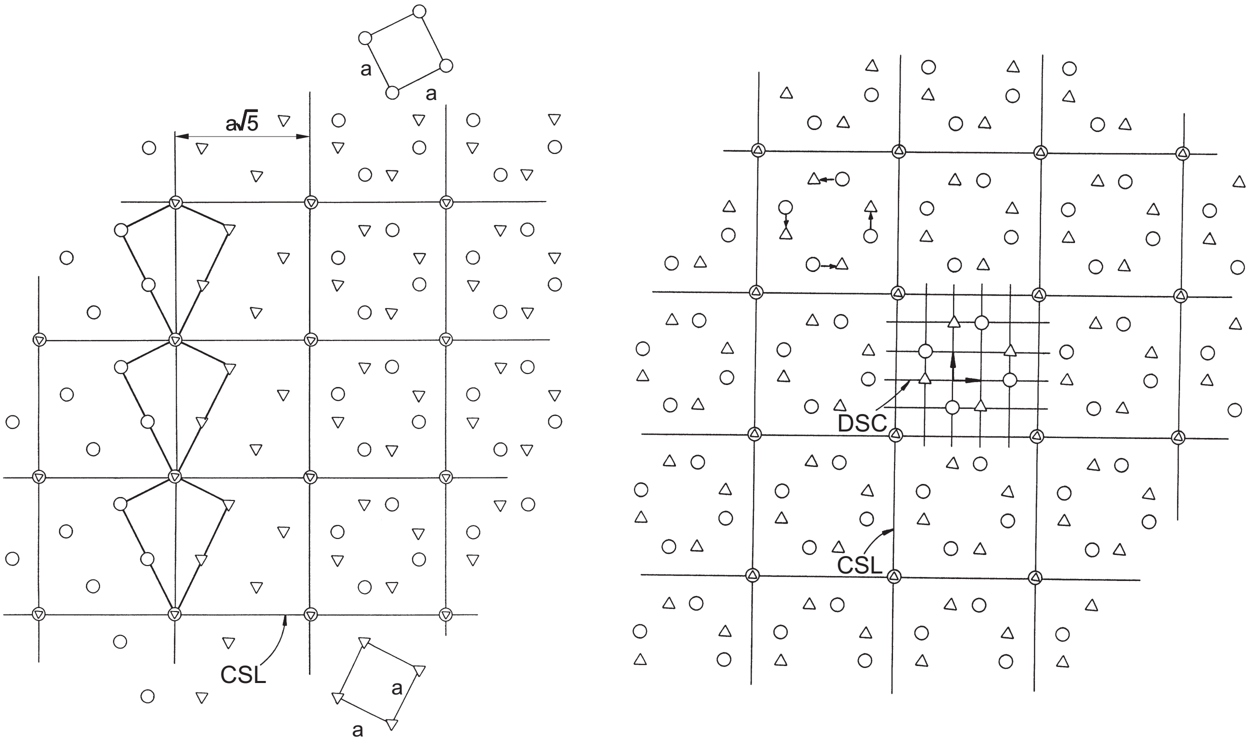

(a) (b)

Fig. 1.4: (a) Coincidence site lattice (CSL) of a 36.87° <100> (Σ=5) grain boundary in a cubic crystal lattice. Left side: grain boundary plane ⊥ plane of the paper (tilt grain boundary); right side: grain boundary plane // plane of the paper (twist grain boundary); (b) Coincidence site lattice (CSL) and displacement shift complete lattice (DSC lattice) at a 36.87° <100> rotation in a cubic crystal lattice. [Gottstein 2010a].

Apparently the elementary cell of the CSL is larger than the elementary cell of the crystal lattice, the density of the CSL lattice with respect to the density of the crystal lattice is measured by the defined quantity Σ

$$\Sigma = \frac{\text{volume of elementary cell of CSL}}{\text{volume of elementary cell of crystal lattice}} \tag{1.4}$$

The quantity Σ defines the similarity between the CSL and the crystal lattices. The smaller Σ is, the more ordered is the grain boundary. Grain boundaries, the misorientation of which is corresponding to a high density of coincidence sites, are called CSL boundaries or special boundaries.

In the case of the 36.87° <100> rotation, $\Sigma = \frac{a(a\sqrt{5})^2}{a^3} = 5$. Low angle grain boundaries can be characterized by Σ=1, since all lattice sites are coincidence sites except for the atoms of dislocation cores. Typical low Σ values with respect to the rotation angle/axis are listed in Table 1.1.

Table 1.1 Table of CSL values in rotation angle φ /axis <uvw>.

<100>		<110>		<111>	
φ	Σ	φ	Σ	φ	Σ
8.80	85	16.10	51	9.40	37
10.39	61	20.05	33	13.20	19
12.68	41	22.80	51	15.20	43
14.25	65	26.57	19	16.40	49
16.26	25	31.59	27	17.90	31
18.92	37	38.94	9	21.78	21
22.62.	13	44.00	57	27.79	13
25.06	85	46.00	59	32.20	39
25.99	89	50.47	11	28.21	7
28.07	17	55.87	41	43.57	49
30.51	65	58.99	33	46.82	19
31.89	53	70.50	3	50.57	37
36.87	5	80.60	43	60.00	3
41.11	73	82.90	57		
42.08	97	86.60	17		
43.60	29				

Geometrically, a CSL only occurs for very special misorientations, any tiny deviation from the exact rotation relationship causes the long range coincidence lost. In the case of non-special grain boundaries, such deviations can be compensated by dislocations with displacement vectors which conserve the size of the CSL as the location of the coincidence sites is allowed to change. These displacement vectors define the Displacement Shift Complete lattice (DSC lattice), Fig. 1.4b, which is the coarsest grid that contains all lattice points of both crystal lattice. Dislocations containing the DSC-lattice vectors as Burgers vectors are referred to as Secondary Grain Boundary Dislocations (SGBDs), in contrast to primary grain boundary dislocations (crystal lattice dislocations). Hence, a general high angle grain boundary can be treated as a deviation from the nearest CSL grain boundary which is compensated by secondary grain boundary dislocations.

1.2.2 Grain boundary energy

The grain boundary energy is sensitive to the eight parameters which describe a grain boundary, especially the five macroscopic parameters, i.e. the orientation relationship and the inclination of the grain boundary. The dependency of the grain boundary energy on the inclination for a constant orientation relationship is commonly presented in the “Wulff plot”, which reveals the positions where the grain boundary energy is considerably low, Fig. 1.5 [Gottstein 2001].

The grain boundary energy is also a function of the orientation relationship between the two crystal lattices. An example of the grain boundary energy dependency on the angle of rotation of a <110> rotation axis in aluminum is given in Fig. 1.6 for symmetrical tilt grain boundaries. Apparently, there are certain orientation relationships with particularly low boundary energy, which correspond to more structurally ordered special grain boundaries (low Σ grain boundaries).

The free energy of a low angle grain boundary can be calculated exactly based on the dislocation model. The stress field of a dislocation in an infinite periodic arrangement is confined to a range in the order of the dislocation spacing *d*. In the case of an edge dislocation its energy per unit length is given as:

$$E_d = \frac{\mu b^2}{4\pi(1-\upsilon)} \ln\frac{d}{r_0} + E_c \tag{1.5}$$

where υ is the Poisson radio, μ is the shear modulus, b is the Burgers vector, $r_0 \approx b$ is the radius of the dislocation core and E_c is the energy of the dislocation core.